(I3) THE USE OF RPC-METAL COMPOSITE FOR SEISMIC ENERGY DISSIPATION DEVICE

Jenn-Chuan CHERN[1] and Yen-Jui CHEN[2]

[1]Distinguished Professor, National Taiwan University, Taipei, Taiwan.
E-mail:jcchern@ntu.edu.tw
[2]Ph.D., Dept. of Civil Eng., National Taiwan University, Taipei, Taiwan.
E-mail:civilche@ms14.hinet.net

Reactive Powder Concrete (RPC) is a kind of high-strength and high-performance cement-based composite. The steel welded wire mesh reinforced thin reactive powder concrete plate (WMRPC) and RPC composite plate (RPCCP) have been fabricated to explore its behavior of energy dissipation subjected to reversed cyclic bending. The fabrication process of plates for the energy dissipation element has also been improved to control distribution, orientation and uniformity of steel fibers in the matrix of WMRPC and RPCCP to reach higher energy dissipation capacity. In this paper, the studies about the effect of steel welded wire mesh, metallic plate and volume fractions of steel fibers on energy dissipation of RPC plate are studied. Under both the monotonic static bending tests and the reversed cyclic bending tests, flexural strength, toughness, and energy dissipation ability of WMRPC and RPCCP are reported. The WMPRCs and RPCCPs are further arranged to become the energy dissipation system (EDS) element for the testing of its mechanical behavior under cyclic loading. A structural analysis was performed to examine the effect of installing a RPC EDS to the frame system for passive structural seismic control. The experimental results indicate that the surfaces of RPCCP flexural plates show multiple cracks and the load versus mid-span deflection curves display the pseudo-displacement-hardening phenomenon and stable hysteretic loops that enhances the ability of energy dissipation. The RPC energy dissipation element provides a superior alternative replacement for metal element in seismic passive structural control engineering applications.

Key Words : *RPC, steel fibers, seismic control, energy dissipation, concrete*

1. INTRODUCTION

Conventional structures use the ductile capacities of its structural members to suppress the input of seismic force without causing the failure of members due to the exceeding of member ductility capacity. There are new technologies developed to control the dynamic behavior of structures and to relieve the seismic force to the major structural members subjected to strong seismic actions. These structural seismic control technologies are categorized as active, passive and hybrid control systems. The passive control system is used to dissipate the input energy from earthquake to avoid the damage to the main structural members. Seismic isolation and passive energy dissipation systems are commonly used for the passive seismic control of structures. For passive energy dissipation system, it usually provides the supplemental damping to the structural system and to reduce the structural response to earthquake motions. A structure can dissipate a large portion of the seismic input energy through inelastic deformations or friction in the energy dissipation devices. In Taiwan, two types of energy dissipation systems are often used, which are hysteretic type and velocity type dampers. The hysteretic dampers include the triangular added stiffness and damping damper (TADAS), reinforce ADAS damper (RADAS), low yield steel shear panel (LYSSP) and Buckling Restrained Braces (BRB) etc. Most of these systems are metallic yielding devices. For velocity type, there are viscoelastic dampers (VE), viscous damper (VD) and viscous damping wall. Viscous fluids and viscoelastic materials are used for the damping subjected to earthquake loading. In general, cement-based materials, including mortar and concrete, exhibit brittle nature. For general reinforced concrete structural designs, the tensile strength of concrete is ignored. Although the compressive strength of concrete is good, it exhibits brittle failure and collapse quickly on reaching the ultimate compressive strength. To improve this drawback, fibers with ductile characteristics are added into these cement-based composites to enhance plastic deformability and energy absorbing capacity by the bridging effect of fibers that resists cracks from further development. (Li 2002)

In recent years, there are some research and applications of using cementitious materials for the application as the damping and energy dissipation systems. Fikuyama and Suwada (2003) developed the HPFRCC damper using the fibrous concrete and reinforcements. Kesner and Billington (2003) developed the DFRCC infill system to act as the shear energy dissipation wall in the structure. Nagai et al. (2003) used the PP-fibers to produce ECC Cementitious composites materials and use that for the PVA-ECC shear wall energy dissipation system. The Kajima Construction Company has developed the ECC using PVA fibers and applied for the tall building constructions since 2000. Xia and Naaman (2002) used the steel fiber reinforced SIFCON as the damping materials and developed the FRC Damper Element shear wall dissipation system.

RPC is a high-strength and high-performance cement-based composite based on micro-structural enhancement techniques.(Richard and Cheyrezy, 1995; Cheng 2003) The compressive strength of the range is between 200 MPa (29 ksi) and 800 MPa (116 ksi). The enhancement of mechanical properties has been achieved through some methods. The improvement of uniformity has been achieved by the elimination of coarse aggregates. The density has been enhanced due to optimal aggregate size grades. The capacity of toughness has been enhanced by incorporation of steel fibers. The improvement of microstructure has been achieved by the use of high temperature curing process. Therefore, RPC has excellent properties including high compressive strength, high flexural strength, high toughness, and increased durability compared to ordinary cement-based materials. RPC has been applied not only to buildings and civil construction, but also to military defense works in some developed countries (Dugat, Roux, and Bernier, 1996). Compared with metals for energy dissipation materials, RPC has the following superior features: (1) has only 1/3 weight to the steel; (2) can be prepared either in precast or in-situ casting to meet the versatile requirements of the construction; (3) can be easily designed and composited with other materials to achieve the desire properties; (4) has higher durability and low maintenance fee (no corrosion and fire protection problem).

In past years, RPC has been studied extensively about its material and structural behavior at National Taiwan University (Chern et al, 2006). From the design principle and the mechanical behavior of composite structure, there still exists opportunity to explore advanced properties of RPC through better production process and improvement of its composite structure. To develop ultra-high-strength and high-toughness structural elements to resist the reversed cyclic loads, WMRPC were fabricated with two dimensional distributed steel fibers and layers of welded wire mesh by pouring of the RPC matrix and placement of steel welded wire meshes in alternate layers. Under the monotonic static bending tests and the reversed cyclic bending tests, first-crack strength, ultimate flexural strength, toughness, stability of hysteretic loops, and energy dissipation ability of WMRPC were investigated (Chern and Chen, 2006b; Chen and Chern et al. 2007). Three metal plates, including steel, aluminum alloy, and lead, were further added to the composite structure of WMRPC to form the RPC composite plate (RPCCP) (Chen and Chern et al., 2006a). The aluminum alloy plate was selected among three metallic plates for this study due to its higher accumulated energy dissipation and its better composite behavior with RPC. The aim of this study focuses on the development of a passive seismic energy dissipation device using RPCCP for structural applications.

2. MATERIALS

The ingredients of RPC matrix include ASTM type II Portland cement [15.8 μm average grain size] ; fine quartz sand [200 μm – 600 μm, 367.5 average grain size]; crushed quartz powder [8.3 μm average grain size]; undensified silica fume [0.37 μm average grain size]; water, and the acrylic graft-copolymer ASTM Type G superplasticizer. The mixture proportions of the ingredients of RPC are listed in **Table 1**.

Table 1 The Mixture Proportions of the Ingredients of RPC.

Plate type	Specific Weight	Yielding strength (MPa)	Tensile strength (MPa)	Elastic modulus (GPa)
Steel	7.8	245	280	200
Aluminum alloy	2.7	34	100	50
Lead	11.3	-	14	1.4

The reinforcements of WMRPC included steel fibers and the steel welded wire meshes. The aspect ratio (length/diameter) of steel fiber [13 mm in length and 0.2 mm in diameter] used was 65. The cross section was round and the shape was straight. Its tensile strength was 2600 MPa. According to the experimental studies (Chern and Chen et al., 2006b), energy dissipation capacity of the WMRPC that reinforced with four layers of steel welded wire meshes and 2% volume fraction of steel fibers was the optimal. The parameters of volume fraction fibers in this study were 2%. The steel welded wire mesh used was 0.8 mm in diameter and 12.7 mm in square mesh size. Its yielding strength of wire mesh was 320 MPa. Four layers of the steel welded wire meshes were used in one specimen in the flexural tests. Aluminum alloy plate with 5 mm thickness was used for studies. Twenty four 20 mm diameter circle holes were drilled and arranged for the passing of matrix and to provide the physical bond between aluminum alloy plate and RPC. The mechanical properties of metallic plates are listed in **Table 2**.

Table 2 Mechanical Properties of Metallic Plates.

Plate type	Specific Weight	Yielding strength (MPa)	Tensile strength (MPa)	Elastic modulus (GPa)
Steel	7.8	245	280	200
Aluminum alloy	2.7	34	100	50
Lead	11.3	-	14	1.4

3. PLATE SPECIMENS AND RELATED TESTINGS

(1) Preparation of plate specimens

The specimen for compression testing was cylindrical, 50 mm in diameter and 100 mm in height. The dimensions of the specimen of flexural testing were 490 mm in length, 150 mm in width, and 35 mm in thickness. The layouts of steel welded wire meshes and metallic plates in the specimen of flexural test are shown in **Fig. 1**. The fabrication process of WMRPC and RPCCP is that, at first we poured the RPC matrix for the first layer, secondly either a piece of steel welded wire mesh or metal plate was put on the surface of the RPC matrix, then continued to pour the second layer of the RPC matrix and repeated the previous steps to the end. Due to the fabrication process, steel fibers could distribute homogeneously between these different steel welded wire mesh layers and metal plates.

All specimens were de-molded 24 hours after the casting and cured for 3 days. The condition for curing was constant at 85℃ and 90% RH. After the high-temperature curing, the specimens were kept at an environment of 20℃ and 90% RH until testing. Compressive and flexural tests were conducted at the age of 7 days.

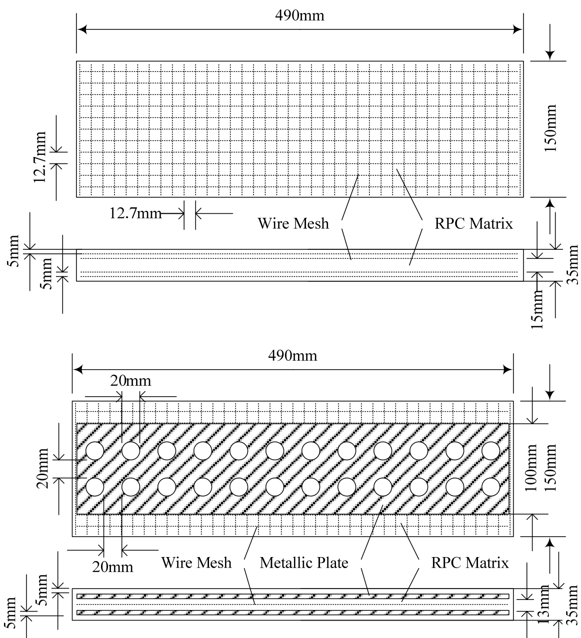

Fig. 1 Dimensions of Flexural Specimen and Layout of Wire Meshes and Metallic Plates.

(2) Experimental studies

The flow table test was carried out according to ASTM C 230/C 230M-98 to confirm the flow ability of the fresh RPC matrix. The compression test was carried out according to ASTM C 39/C 39M-99. The experimental program of flexural test included flexural strengths, toughness indices, and residual strength factors to ASTM C 78-94 and C 1018-97. The consistent results were obtained through the proofs of repeated tests using the setups. Two linear variable differential transformers (LVDT) were installed at the mid-span positions of the lateral sides of specimen to measure mid-span deflections. The loading was displacement controlled by the material test system (MTS). The load versus mid-span deflection curve was continuously recorded during the entire test. The pseudo-static reversed cyclic bending history called R1 was selected for the test, as shown in **Fig. 2**. In the R1 loading history, the period of every complete loading cycle was 20 seconds (i.e. 0.05 Hz loading frequency). At the same amplitude of loading, the process repeated twice. The increasing increment of loading amplitude was to take the method of arithmetic series. The incremental value was 0.2 mm. The main purpose was to obtain the complete behavior of hysteretic loops.

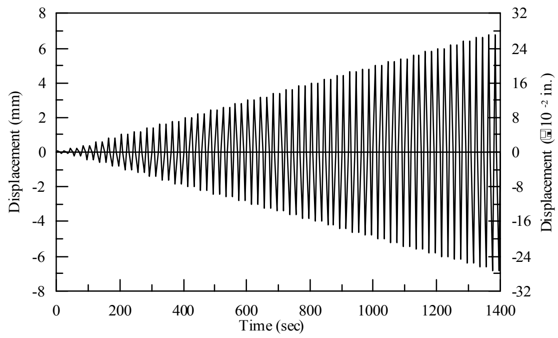

Fig. 2 R1 Loading History.

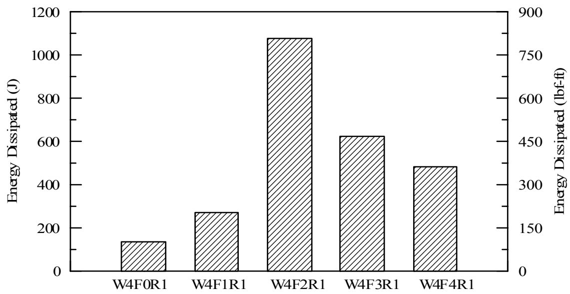

Fig. 4 Accumulated Energy Dissipation of Specimens with Different Fiber Contents.

(3) Results and discussion

In the flow table tests of the fresh RPC matrix, the average values of slump flow were 23 cm when adding 2% volume fractions of steel fibers. In the compression tests of the hardened RPC with 2% volume fibers fraction, the average value of compressive strength was 180 MPa.

By investigating the experimental results subjected to R1 loading history in this study, the optimal volume fraction of steel fiber with four layers of steel welded wire meshes in the WMRPC specimen was based on accumulated dissipated energy. The hysteretic loops for 2% volume fractions of steel fiber in WMRPC are shown in **Fig. 3**. The average ultimate-flexural strengths were 5.4 MPa, 15.4 MPa, 25.5 MPa, 32.4 MPa, and 38.1 MPa for specimens containing 0%, 1%, 2%, 3%, and 4% volume fraction of steel fibers respectively. All cases above, except specimen with 0% fibers, showed an interval of pseudo-displacement-hardening region. It can be concluded that the growth of ultimate-flexural strength was due to the increase of volume fraction of steel fiber in WMRPC.

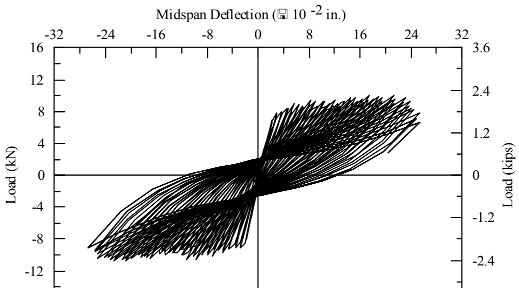

Fig. 3 Hysteretic Loops of W4F2.

The comparison of accumulated dissipated energy is shown in **Fig. 4**. W4F2 (4 layers wire meshes and 2% fiber content) performed better than other specimens with 1%, 3% and 4% fiber volume fractions and the average value was 1079 J. By comparing the area of single loop of hysteretic curves, W4F2 exhibited fuller loops than others.

While under reversed cyclic bending, the results of accumulated dissipated energy shown in **Fig. 5** shows that W4F0 (0%) was approximately 134 J. In the case of W0F2R1, only reinforced with 2% volume fraction of steel fibers, the accumulated dissipated energy was approximately 752 J. Not unexpectively, the accumulated energy 1079 J of W4F2R1 that reinforced with 4 layers of steel welded wire meshes and 2% volume fraction of steel fibers was 193 J higher than the sum of the previous two cases. Therefore, the addition of four layers of steel welded wire meshes can increase the dissipated energy by 40% compared to that of the specimens reinforced only with 2% volume fraction of steel fibers. W4F2, which can enhance the ultimate flexural strength and energy dissipation capacity under reversed cyclic bending effectively, will be used as the basic mix for further improvements with the incorporation of metallic plates.

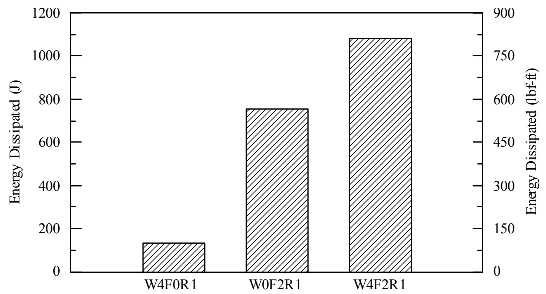

Fig. 5 Accumulated Energy Dissipation of W4F0, W0F2, and W4F2 under Reversed Cyclic Bending.

There were three metallic plates used for the tests, which are steel, aluminum alloy and lead (**Table 3**). Chen and Chern (2006a) have shown that AL2F2 was found to have superior performance of in extensibility as compared to other specimens. The toughness 216J of AL2F2 is roughly equal to 224J of ST2F2 despite that the strength of steel plate is much higher than aluminum plate and the ultimate flexural strength of ST2F2 is 70% higher than that of AL2F2. The toughness index for WM2F2, ST2F2, AL2F2 and LE2F2 are 12.7, 13.2, 18 and 11. Based on former findings, AL2F2 has wider pseudo-displacement hardening zone and stable loading range with higher toughness. For ST2F2 specimen, the strength decreases rapidly upon its reach to the peak of curve. The wider cracks due to the fast localization of microcracks in RPC were observed in the specimen during the loading process. .The residual strength of ST2F2 depends solely by the tensile strength of steel plates. AL2F2 demonstrated better mechanical behavior with good deformational compatibility between aluminum plates and RPC. The densely distributed multiple microcracks were developed and progressed gradually into stable major cracks on the surface of RPC. This stable fracture process made AL2F2 possess much higher pseudo-displacement hardening zone and with higher toughness. The close value of elastic modulus of aluminum alloy 50 GPa to that of RPC 45 GPa is the major factor of higher compatibility for this composite plate.

Table 3 Specimens with Different Designs and the Loadings.

Items / Specimens	W : Steel wire mesh layers ST : Steel plate layers AL : Aluminum alloy plate layers LE : Lead plate layers	F : Fiber volume fraction (%)
W4F2	4	2
ST2F2	2	2
AL2F2	2	2
LE2F2	2	2

Table 4 Results of Reversed Cyclic Bending Tests.

Mixture No.	WM4F2	ST2F2	AL2F2	LE2F2
U. F. S. D. (mm)	2.8	3.0	3.1	2.2
U. F. S. (MPa)	25.5	71.5	40.4	19.7
A. D. E. (J)[1]	1079	1920	2462	1628

[1] A. D. E. : Accumulated Dissipation Energy
[2] U. F. S. D. : Ultimate Flexural Strength Deflection
[3] U. F. S. : Ultimate Flexural Strength

The hysteretic loops of load versus mid-span deflection of AL2F2 subjected to reversed cyclic bending load are shown in **Figure 6(a)**. The average ultimate flexural strength and corresponding deflection, and the accumulated dissipation energy before failure of test specimens are listed in **Table 4**. Since the RPCCP in essence is cementitious composite, it shows the strength degradation, stiffness degradation and the necking response in hysteretic loading process. While the use of different reinforcing metallic materials demonstrated various load versus deflection response. The ultimate flexural strength of W2F2, ST2F2, AL2F2 and LE2F2 are 25.5 MPa, 71.5 MPa, 40.4 MPa and 19.7 MPa, respectively. The trend of magnitude of ultimate flexural strength of the specimens subjected to cyclic loading is similar to that under monotonic loading; however all cyclically loaded specimens have only 70% of ultimate strength to that under monotonic loading. The single hysteretic loop of AL2F2 shows the better full bounding which incorporates much larger energy dissipation area and results in much less shrinking phenomenon of hysteretic curve. The accumulate dissipation energy of W2F2, ST2F2, AL2F2 and LE2F2 are 1079J, 1920J, 2462J and 1628J. The AL2F2 has the highest energy dissipation capacity under cyclic loading. Bases on previous studies, we can conclude that AL2F2 can provide better toughness and energy capacity under cyclic loading.

The AL2F2 composite was made by the adding of steel fibers and aluminum alloy plate. The major energy dissipation mechanism comes from the pull-out and microcrack suppression capability of short steel fibers in RPC matrix and the higher ductility of aluminum alloy plate. The failure state of AL2F2 is shown in **Fig. 6**. The very large mid-span deflection can be achieved as shown in **Fig. 6(b)**. The surfaces of specimens of W4F2 showed tight multiple micro-cracks, one or two main cracks could occur when loading continuously until broke in one main crack. Due to the crack resisting effect of steel fibers and steel welded wire meshes, multiple-cracks means that much more energy can be dissipated and delays the development of unstable situation. During the loading process, the longitudinal steel wires were stretched to contribute strain energy, and the transverse steel wires helped to restrain the development of multiple cracks speedily and eliminate the phenomenon of cracking localization. Steel welded wire meshes (the yielding strength is 320 MPa) would yield and break at the ultimate stage. Then the specimens exhibited tensile collapse pattern. On the other hands, the tensile strength of steel fibers, 2600 MPa, is much higher than the stress between matrix and steel fibers as the steel fibers during fiber pull out process. The situations of steel welded wire meshes yielding and breaking, and steel fibers pulling out, can be observed by tested specimens as shown in **Fig. 6(c)**. Therefore, steel fibers provided a frictional mechanism to dissipate the loading energy. Furthermore, due to the development of multiple cracks, steel fibers could contribute to more energy dissipation during the pull out process. The energy dissipated by the frictional process during pull out process of the fibers bridging each crack multiplied as the number of cracks increased. The existence of longitudinal wires provided important effect in uniform stress distribution in specimen and, thus, allowed multiple cracking to occur. At the final fracture stage, the aluminum plate yields up to breaking and the steel fibers were pulled out in the fracture cleavage (**Fig. 6(c)**, **Fig. 6(d)**). The excellent deformational compatibility between RPC and aluminum due to their close modulus of elasticity value contributes to the material excellence for higher ductility and energy dissipation of AL2F2.

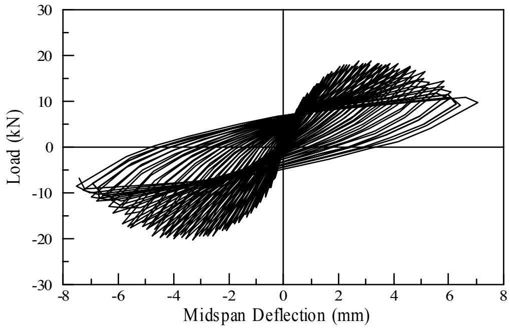

(a)

(b)

(c)

(d)

Fig. 6 Experimental Results of AL2F2 (a) Hysteretic Loops , (b) Deflection Curve, (c) Yielding and Breaking of Aluminum Alloy Plate, and (d) Pulling Out of Steel Fibers.

4. RPC ENERGY DISSIPATION DEVICE

An EDS is designed as the axial member to be installed in the structure. The function of EDS develops through the deformation of RPCCPs under flexural loading. **Fig. 7** shows a typical unit of EDS which is composed of metal fixture and RPCCPs made of AL2F2. An EDS two force member model is shown in **Fig. 8**. Chen (2006) has found that the ultimate strength and accumulated dissipation energy increases as the loading frequency increases from 0.05 Hz to 0.2 Hz. The number of plates and their dimension can be engineering designed to meet the structural requirement. The EDS was tested using MTS servo-controlled testing machine for its mechanical behaviors. **Fig. 9(a)** shows the load versus deflection hysteric loops of EDS made of 4 pieces RPCCP. The ultimate flexural strength (U.F.S.), and accumulated dissipation energy (A.D.S.), and unit volume dissipation energy (U.V.D.E.) of EDS device with four WMRPCs and AL2F2 RPCCPs are listed and compared in the **Table 5**. The U.V.D.E. of AL2F2 is 2.8 times higher than that made of WMRPC.

Table 5 The Comparison of Strength and Energy Behavior between EDS Devices Made of WMRPCs and AL2F2s.

Specimen No.	U.F.S. (MPa)	A.D.E. (J)	U.V.D.E. (J/m^3)
W4F2	24.6	5711	971292
AL2F2	34.8	15992	2719770

[1] U.F.S. ：Ultimate Flexural Strength
[2] A.D.E. ：Accumulated Dissipation Energy
[3] U.V.D.E. ：Unit Volume Dissipation Energy

Fig. 7 Setup of AL2F2 EDS Device under Testing.

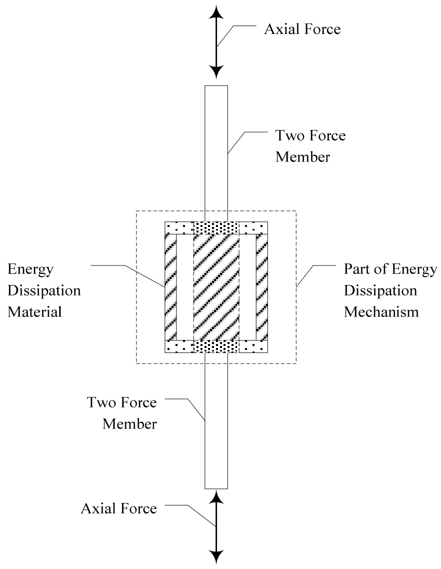

Fig. 8 A Model for EDS Energy Dissipation Two Forces Member.

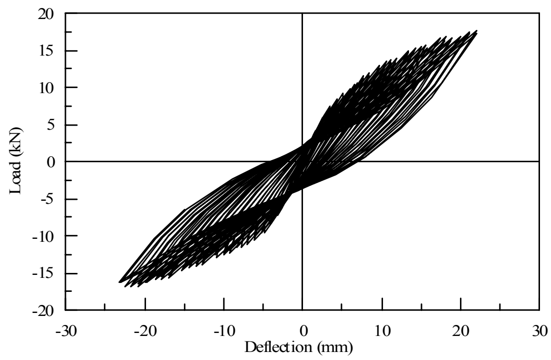

(a)

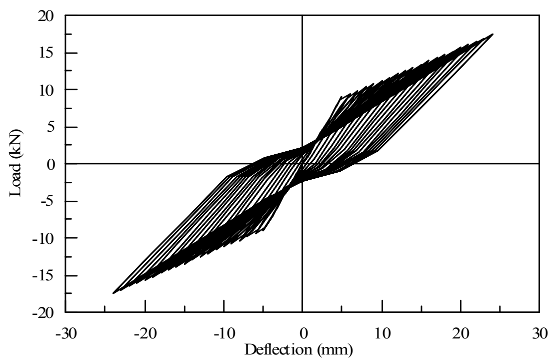

(b)

Fig. 9 Hysteric Loops of AL2F2 EDS Device under Reversed Cyclic Loading: (a) Experimental Result, (b) Numerical Modeling.

5. FRAME ANALYSIS WITH DISSIPATION DEVICE

For numerical study, SAP2000N program was used for frame analysis by inputting the basic mechanical properties obtained from the experimental results of EDS. The hysteric loops of EDS can be modeled as three stages: the first stage is elastic behavior; the second stage starts to display pseudo-displacement-hardening phenomenon behavior as the EDS plate reaches the initial crack; the strain-softening response develops at third stage as the displacement increases after attaining the peak load. This analysis uses the multi-linear plastic model (Pivot model) of Nonlinear Link to simulate the shape and characteristics of hysteric loops. The characteristic of hysteric loops includes strength reduction, stiffness degradation and slippage phenomenon. The numerical simulation of the hysteric loops of EDS is shown in the **Fig. 9(b)** as compared to that of the experimental result in **Fig. 9(a)**. The comparison shows that the modeling of shape of hysteric loops is quite similar to the experimental result. The numerical modeling on the accumulated dissipation energy is 3900 J which is also close to the experimental result 3912 J with only 0.3% error.

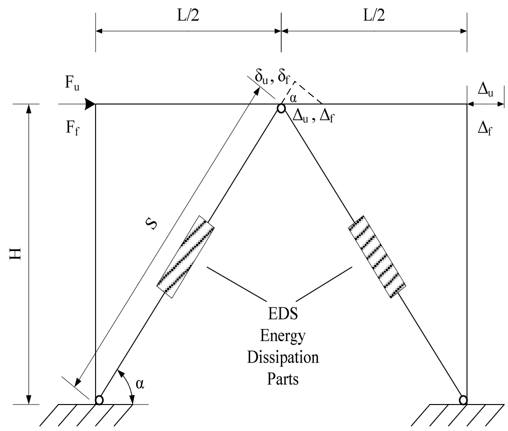

Fig. 10 Frame with EDS Device for Numerical Analysis.

Comparative numerical studies were further performed to study the structural behavior of pure frame and the frame with the installation of two EDSs subjected to reversed cyclic loading with 0.05 Hz. The height of column is 4 m and the span is 8 m (**Fig. 10**). H shape H400x400x12x20 steel members were used both for columns and beam with A36 steel. 24 dissipation plates were used for each EDS link member. The structural analysis shows that the plastic hinge develops at the bottom of a column in 456 seconds which leads to the large side sway and then the instability of the pure frame structure. The numerical analysis of the frame with EDSs shows that the frame went through the 500 seconds loading history without failure. During the analysis, an EDS falls into the nonlinear stage in 205 seconds. As the lateral load increases, the EDS links take more axial force and start to dissipate energy. As the frame takes the largest lateral load 600 kN, the lateral load resistance taken by EDSs is 127 kN and the 9000 J energy is dissipated. The analysis reveals the function of EDS device which provides both structural stiffness and energy dissipation function to the structural system.

6. CONCLUSIONS

RPCCP provides a good alternative to metals as a material for design to resist reversed cyclic loading. The high toughness and energy dissipation capacity properties were achieved through the design and manufacture of metallic reinforced reactor power concrete composite plates. This study shows that the surfaces of AL2F2 specimens show multiple cracks and the load versus mid-span deflection curves display the pseudo-displacement-hardening phenomenon and stable hysteretic loops, thus enhances the ability of energy dissipation. The good deformational compatibility between aluminum alloy and RPC contributes to the success of high energy adsorption response. The EDS made of RPCCPs can be installed in the structure and proved to provide both stiffness and energy dissipation capacity to the structural system.

ACKNOWLEDGMENT: The authors are grateful for the financial support of the National Science Council of Taiwan under Grants: NSC 95-2221-E-002-413.

REFERENCES

1) Chen, Y. J. : The Research and Application on Energy Dissipation Behavior of Composite RPC Members, *Ph.D. Dissertation*, National Taiwan University, Taipei, Taiwan, 2006.
2) Chen, Y. J., Chern, J. C., and Chan, Y. W., et al. : Reinforced Reactive Powder Concrete Plate under Cyclic Loading, *Journal of the Chinese Institute of Engineers*, Vol. 30, No. 2, pp. 299-310, 2007.
3) Cheng, R. B. : Study of Mechanical Properties of Reactive Powder Concrete Structural Members, *Ph.D. Dissertation*, National Taiwan University, Taipei, Taiwan, 2003.
4) Chern, J. C., et al. : The Development, Applications, and Outlook of Super-High Performance Concrete RPC, *Proceedings of the eighth National Conference on Structural Engineering*, Yuenlin, Taiwan, 2006.
5) Chern, J. C. and Chen, Y. J. : Experimental Study on Cyclic Performance of Metal Reinforced Reactive Powder Concrete Plate, *The 2nd fib Congress*, June 5-8, Naples, Italy, 2006a.
6) Chern, J. C. and Chen, Y. J. : Study of Energy Dissipation Capacity of Reactive Powder Concrete Plate, *2nd ACF International Conference*, 20-21 Nov., Bali, Indonesia, 2006b.
7) Dugat, J., Roux, N., and Bernier, G. : Mechanical Properties of Reactive Powder Concretes, *Materials and Structures*, Vol. 29, pp. 233-240, 1996.
8) Fukuyama, H. and Suwada, H. : Experimental Response of HPFRCC Dampers for Structural Control, *Journal of Advanced Concrete Technology*, Vol. 1, No. 3, pp. 317-326, 2003.
9) Kesner, K. E. and Billington, S. L. : Experimental Response of Pre-cast Infill Panel Connections and Panels Made with DFRCC, *Journal of Advanced Concrete Technology*, Vol. 1, No. 3, pp. 327-333, 2003.
10) Li, V. C. : Large Volume, High-Performance Applications of Fibers in Civil Engineering, *Journal of Applied Polymer Science*, Vol. 83, pp. 660-686, 2002.
11) Nagai, S., Kanda, T., Maruta, M., and Miyashita, T. : Shear Capacity of Ductile Wall with High Performance Fiber Reinforced Cement Composite, *Proceedings of the 1st fib Congress*, Session 6, pp. 767-774, 2003.
12) Richard, P. and Cheyrezy, M. : Composition of Reactive Powder Concretes, *Cement and Concrete Research*, Vol. 25, No. 7, pp. 1501-1511, 1995.
13) Xia, Z. and Naaman, A. E. : Behavior and Modeling of Infill Fiber-Reinforced Concrete Damper Element for Steel-Concrete Shear Wall, *ACI Structural Journal*, Vol. 99, No. 6, pp. 727-739, 2002.